Accelerated increases in global and Asian summer monsoon precipitation from future aerosol reductions

Laura J. Wilcox[1,2], Zhen Liu[3], Bjørn H. Samset[4], Ed Hawkins[1,2], Marianne T. Lund[4], Kalle Nordling[5], Sabine Undorf[6], Massimo Bollasina[3], Annica M. L. Ekman[6], Srinath Krishnan[6], Joonas Merikanto[5], and Andrew G. Turner[1,2]

[1]National Centre for Atmospheric Science, UK
[2]Department of Meteorology, University of Reading, Reading, UK
[3]School of Geosciences, Grant Institute, University of Edinburgh, Edinburgh, UK
[4]CICERO Center for International Climate and Environmental Research, Oslo, Norway
[5]Finnish Meteorological Institute, Helsinki, Finland
[6]Department of Meteorology, Stockholm University, Stockholm, Sweden

Correspondence: Laura Wilcox l.j.wilcox@reading.ac.uk

Abstract. There is large uncertainty in future aerosol emissions scenarios explored in the Shared Socioeconomic Pathways (SSPs), with plausible pathways spanning a range of possibilities from large global reductions in emissions to 2050 to moderate global increases over the same period. Diversity in emissions across the pathways is particularly large over Asia. Rapid anthropogenic aerosol and precursor emission reductions between the present day and the 2050s lead to enhanced increases in

5   global and Asian summer monsoon precipitation relative to scenarios with weak air quality policies. However, the effects of aerosol reductions don't persist in precipitation to the end of the 21st century, when response to greenhouse gases dominates differences across the SSPs. The relative magnitude and spatial distribution of aerosol changes is particularly important for South Asian summer monsoon precipitation changes. Precipitation increases here are initially suppressed in SSPs 2-4.5 and 5-8.5 relative to SSP 1-1.9 and 3-7.0 when the impact of East Asian emission decreases is counteracted by that due to continued

10   increases in South Asian emissions.

1   Introduction

Anthropogenic aerosols can affect climate either by scattering or absorbing solar radiation, or by changing cloud properties (Boucher et al., 2013). Overall, aerosols have a global-mean cooling effect, manifested, for example, in a slower rate of global

15   warming in the mid twentieth century concurrently with the rapid increases in aerosol burden (Wilcox et al. (2013); Jones et al. (2013); Hegerl et al. (2019)). This has raised the question of whether the warming associated with present-day and future reductions in anthropogenic aerosol might exacerbate the climate impacts brought about by continued increases in greenhouse gas emissions alone.

Many studies have demonstrated the potential for an enhanced future warming from aerosol reductions in global climate models driven by plausible reductions in the emissions of anthropogenic aerosol and their precursors (e.g. Chalmers et al. (2012); Levy et al. (2013); Rotstayn et al. (2013); Acosta Navarro et al. (2017)), which in recent years have typically been taken from either the Representative Concentration Pathways (RCPs; Moss et al. (2010); van Vuuren et al. (2011)) used in

5   the 5th Coupled Model Intercomparison Project (CMIP5; Taylor et al. (2012)), or the more diverse ECLIPSE (Klimont et al., 2017) aerosol pathways: CLE (Current LEgislation), and MFR (Maximum Feasible Reductions). Estimates based on transient simulations with CMIP5 generation models suggest that future aerosol reductions may result in warming of up 1.1K in addition to any greenhouse gas (GHG)-driven warming (e.g. Rotstayn et al. (2013); Levy et al. (2013); Acosta Navarro et al. (2017)). This means that reduced anthropogenic aerosol emissions may account for up to half of the total warming by 2100 in scenarios

10 with moderate GHG increases. Similar magnitudes are also seen in studies using equilibrium experiments (Kloster et al., 2010), reduced complexity models (Hienola et al., 2018), and studies assuming a complete removal of anthropogenic aerosol (Samset et al. (2018); Nordling et al. (2019)).

The important role of anthropogenic aerosol in driving precipitation changes has also been documented, including the possible contribution to the spin down in the global water cycle in the mid-twentieth century (Liepert et al. (2004); Wilcox et al.

15 (2013); Wu et al. (2013)). A greater response of global mean precipitation to anthropogenic aerosol changes compared to GHGs is expected since shortwave drivers have a stronger influence on the water cycle (e.g. Liepert et al. (2009); Andrews et al. (2010); Rotstayn et al. (2013); Samset et al. (2016); Liu et al. (2018)). The apparent hydrological sensitivity (% change in precipitation divided by absolute change in temperature; Fläschner et al. (2016)) for anthropogenic aerosol is twice that for GHGs (Kloster et al. (2010); Salzmann (2016); Samset et al. (2016)). This enhanced sensitivity means that anthropogenic

20 aerosol reductions might be expected to play a relatively more important role in future increases in global precipitation for a given temperature change. Several studies using CMIP5 models estimate an increase in global mean precipitation between 0.09 and 0.16 mm day^{-1} by 2100 from aerosol reductions (e.g. Levy et al. (2013); Rotstayn et al. (2013); Westervelt et al. (2015)).

Their heterogeneous forcing distribution and influence on circulation patterns mean that the effects of future aerosol reductions are likely to be felt more strongly at regional than global scale. Previous work has identified relatively large temperature

25 increases over Europe (Sillmann et al., 2013), the Arctic (Acosta Navarro et al., 2016), and East Asia (Westervelt et al., 2015), compared to the global mean response. For precipitation, the regional response is particularly pronounced for the Asian summer monsoon (Levy et al. (2013); Westervelt et al. (2015); Acosta Navarro et al. (2017); Bartlett et al. (2018); Samset et al. (2018)). Here, precipitation is sensitivie to changes in remote aerosol through its control on the Interhemispheric Temperature Gradient and Inter Tropical Convergence Zone (ITCZ) location, and to local aerosol changes, which further modify the local monsoon

30 circulation (Polson et al. (2014); Dong et al. (2016); Guo et al. (2016); Shawki et al. (2018); Undorf et al. (2018)). Asia will also undergo the largest anticipated changes in aerosol amounts worldwide (Lund et al. (2018); Scannell et al. (2019)), and is thus a region likely to see an anthropogenic aerosol influence on near-future precipitation trends.

Despite evidence that anthropogenic aerosols influence temperature and precipitation, quantification of the associated changes is hindered by several compounding uncertainties. The degree by which AA reductions enhance future climate change is model

35 dependent, with models featuring weaker historical aerosol forcing generally predicting more moderate global mean warming

(Gillett and Von Salzen (2013); Westervelt et al. (2015)) and precipitation increases due to aerosol reductions in future (Rotstayn et al., 2015). The uncertainty in aerosol radiative forcing itself is currently the largest source of uncertainty in estimates of the magnitude of the anthropogenic forcing on climate, with the most recent estimate producing a 68% confidence interval from $\sim$-1.60 to $\sim$-0.65 W m^{-2} (Bellouin et al., 2019). This is comparable to the range simulated by CMIP5 models: -1.55 to -0.68 W m^{-2} (Zelinka et al., 2014). The effect of this uncertainty on regional climate projections may be further enhanced by feedbacks from circulation changes (Wilcox et al., submitted). The compensating effects from the response to different near-term climate forcers also adds to uncertainty in multi-decadal projections, with future changes in methane and nitrate aerosol having the potential to moderate future temperature enhancements from decreases in anthropogenic aerosol (Bellouin et al. (2011); Shindell et al. (2012); Pietikäinen et al. (2015)).

In opposition to the CMIP5-generation findings summarised above, Shindell and Smith (2019) recently dismissed the possibility that future aerosol reductions might lead to rapid increases in the magnitude or rate of global-mean warming, even in scenarios with aggressive clean air policies, based on simulations with a reduced-complexity impulse response model (Smith et al., 2018). Yet, this conclusion may not hold when using a full coupled GCM and when investigating changes beyond global mean temperature Even if the short atmospheric residence time of anthropogenic aerosol possibly makes their effects negligible on centennial timescales, they are likely important for regional and global climate over the next few decades. This is particularly the case for Asia where large aerosol emission changes are anticipated, and where aerosol has played an important role in historical changes, in particular for precipitation. In this study, we examine state-of-the-art models and scenarios in CMIP6 and make the case for a potential enhancement of increases in global and Asian temperature and precipitation on a 20-30 year time horizon due to anthropogenic aerosol. Such an effect is of particular importance for adaptation measures.

2 Data and methods

2.1 Models and experiments

We use data from CMIP6 (Eyring et al., 2016). At the time of writing, data were only available for between 6 and 14 models for the variables and experiments we consider. The data used in this study are summarised in Table 1. All available data is used for each experiment, except where otherwise stated. Many CMIP6 models include improved representation of aerosol microphysics and aerosol-cloud interactions, such as internal mixing and heterogeneous ice nucleation (e.g. Bellouin et al. (2013); Mulcahy et al. (2018); Kirkevåg et al. (2018); Wyser et al. (2019)). We use data from the historical experiment (1850-2014) and four future scenarios following Shared Socioeconomic Pathways (SSPs) 1-1.9, 2-4.5, 3-7.0, and 5-8.5 (O'Neill et al. (2016); Rao et al. (2017); Riahi et al. (2017)), which sample a range of aerosol pathways.

The SSPs used in CMIP6 sample a far greater range of uncertainty in future aerosol and precursor emissions than the RCPs used in CMIP5 (Scannell et al. (2019); Lund et al. (2018)). Partanen et al. (2018) highlighted the importance of uncertainty in aerosol emission pathways for the potential enhancement of global temperature increases from anthropogenic aerosol reductions. The CMIP5 RCPs 2.6-8.5 sampled only a limited range of this emission uncertainty, with an associated 0.18K difference in global mean temperature. Contrasting aerosol pathways spanning a wider range of emission uncertainty resulted in a 0.86K

difference. The SSPs span most of this wider range explored by Partanen et al. (2018). They consider large, rapid reductions in aerosol and precursor emissions in SSP1-1.9, more moderate reductions (comparable to the RCPs) in SSP2-4.5 and SSP5-8.5, and continued increases in the coming decades in SSP3-7.0 (see Figure 1). Much of the spread in global emission pathways comes from diversity over Asia and North Africa (Lund et al., 2018).

5   In our analysis, we compare the future decadal-mean climate changes to the present day (1980-2014) across SSPs 1-1.9, 2-4.5, 3-7.0, and 5-8.5. We focus on the period up to the 2050s, when aerosol emission uncertainty is largest, but the full range of uncertainty in greenhouse gas (GHG) emissions has yet to be emerge (Figure 1). However, the changes in GHG emissions in this period are not negligible, and the anomalies we show include the effects of changes in both anthropogenic aerosols and greenhouse gases. This precludes the quantification of the respective effects of aerosol and greenhouse gas changes, but does

10   not prevent the identification of the main driver of the anomaly. If the magnitude of the anomaly decreases monotonically from SSP1-1.9, which has the largest aerosol reduction, to SSP3-7.0, which has a moderate aerosol increase (Figure 1), this indicates that aerosol changes are the main driver of the climate response. Further confirmation of aerosol as the main driver is gained from the comparison of the anomalies in SSP2-4.5 and SSP5-8.5, which have similar aerosol pathways, but very different greenhouse gas pathways (Figure 1). If the response in these two scenarios is similar, then the greenhouse gas influence has yet

15   to emerge over the aerosol signal. As the differences in greenhouse gas emissions between the two scenarios increase, a larger response is expected in SSP5-8.5, which has large increases in global GHG emissions compared to very moderate increases in SSP2-4.5 (Figure 1). In cases where GHGs are the main driver of the anomaly, the responses will increase monotonically from SSP1-1.9 to SSP5-8.5.

    In Section 4.1, we use an additional DAMIP (Detection and Attribution Model Intercomparison Project; Gillett et al. (2016))

20   experiment, SSP2-4.5-aer. This differs from the companion SSP2-4.5 in that only aerosol emissions are evolving while all other forcings are held constant at their 1850 levels. This scenario allows the response to anthropogenic aerosols to be seen in isolation from the response to greenhouse gas changes and may thus provide support to any conclusion drawn from the analysis of the SSP2-4.5 experiment. Data for this experiment is so far only available for two models, CanESM5 and MIROC6. In this analysis, decadal mean anomalies are again presented relative to the present day (1980-2014). However, in this case,

25   the present day is necessarily defined based on the historical-aer simulation (a historical simulation where only anthropogenic aerosol and precursor emissions are transient, also included in DAMIP).

2.2   Present day model evaluation

Here, we use a number of observation and reanalysis datasets to present a broad evaluation of the performance of CMIP6 models in reproducing present day (1980-2014) climatologies and linear trends in global temperature and precipitation, the

30   interhemispheric temperature gradient, and Asian summer monsoon. Global temperature observations are taken from GIS-TEMP v4 (Hansen et al. (2010); Lenssen et al. (2019)), the Goddard Institute for Space Studies gridded dataset, which is based on GHCN v4 over land (Global Historical Climatology Network; Menne et al. (2018)) and ERSST v5 over ocean (Extended Reconstructed Sea Surface Temperature; Huang et al. (2017)). GISTEMP is provided as anomalies relative to 1951-1980 on a $2° \times 2°$ grid. For global precipitation, data from the Global Precipitation Climatology Project (GPCP; Adler et al. (2003))

are used on a 2.5° × 2.5° grid. GPCP combines gauge- and satellite-based observations over land with satellite observations over ocean. Since there can be large discrepancies between precipitation observations from different sources (Collins et al. (2013); Sperber et al. (2013); Prakash et al. (2015)), we use a number of datasets in our evaluation of the Asian summer monsoon. Precipitation observations over land are taken from APHRODITE (Asian Precipitation - Highly-Resolved Observational

5   Data Integration Towards Evaluation; Yatagai et al. (2012)) and the Global Precipitation Climatology Centre (GPCC; Schneider et al. (2014)). APHRODITE contains data from a dense network of rain gauges and is used at 0.25° × 0.25° resolution, within the domain bounded by 60°E, 150°E, 15°S, and 55°N. GPCC also provides gauge-based data, but at a reduced horizontal resolution (0.5° × 0.5°) compared to APHRODITE. We also show precipitation from CMAP (Climate Prediction Centre Merged Analysis of Precipitation; Xie et al. (1996); Xie et al. (1997)), which blends satellite and gauge-based estimates with

10   NCEP/NCAR reanalysis precipitation. The atmospheric circulation plays an important role in the distribution of Asian summer monsoon precipitation, so we also compare upper- and lower-tropospheric winds from CMIP6 models to ERA-Interim (Dee et al., 2011).

The global-mean annual-mean temperature anomaly from GISTEMP falls within the range of the CMIP6 ensemble during the historical period (Figure 2a). However, most models overestimate the rate of recent warming (Figure 2e). The interhemi-

15   spheric temperature gradient (Northern Hemisphere - Southern Hemisphere) anomalies are also consistent in GISTEMP and CMIP6 (Figure 2b), although the models generally have anomalies that are more postitive than seen in the observations. Most model members reproduce the negative trend in the interhemispheric temperature gradient in 1950-1974 (Figure 2e), which is associated with a global increase in anthropogenic aerosol and a weakening of the global monsoon (e.g. Polson et al. (2014)). The models also capture the positive trend since 1980-2014 when rates of change in the global aerosol burden were relatively

20   small (Figure 2e).

All models simulate an increase in global-mean annual mean precipitation since 1980, and most members simulate larger trends than observations (Figure 2c,e). The observed trend in Asian (67.5-145°E, 5-47.5°N) summer precipitation is small compared to interannual variability, and this is reflected in large uncertainty in the sign of the modelled trend (Figure 2d, e).

Modelled global mean precipitation for the period 1980-2014 is too large compared with GPCP data, primarily due to

25   excessive tropical precipitation (Figure 2c). The models generally overestimate midlatitude precipitation trends, and show no consensus on the sign of the trend in the SH tropics and subtropics (Figure 2d). However, the models do capture the time evolution of the global precipitation anomaly.

Compared to APHRODITE, the CMIP6 ensemble mean underestimates summer (June-September, JJAS) monsoon precipitation amount over India, and overestimates it over the Tibetan Plateau and the Indo-China peninsula (Figure 3a, c). The

30   magnitude of the bias between the CMIP6 multi-model mean and APHRODITE is comparable to the magnitude of the difference between observational datasets over northeast China and India, but model bias over Tibetan Plateau and Indo-China peninsula is relatively large (Figure 3). The modelled meridional component of the monsoon circulation at 850hPa is too strong over the Equatorial Indian Ocean, while the flow over the Bay of Bengal, and the extension of the circulation into China, is too weak (Figure 3e). This pattern is seen in almost all models, and is highlighted in the comparison of the zonal and meridional

35   components of the 850 hPa wind in CMIP6 and ERA-Interim in Figure 3f. This weak extension of the summer monsoon into

eastern China, with an anomalously strong extension into the subtropical west Pacific is consistent with the pattern of differences between CMIP5 models and observations (Sperber et al., 2013), although the CMIP6 models are more skilful in their representation of the Indian summer monsoon compared to CMIP5 (Gusain et al., 2020).

While aspects of the CMIP6 multi-model mean summer monsoon compare well with observations, and the multi-model mean performs better than the individual models, there is a large inter-model diversity in the monsoon characteristics exhibited (summarised in Figure 3f; maps of present - day means, and anomalies compared to observations are shown for individual models in Supplementary Figures S1-S5). Of the models we will consider on an individual basis in Section 4.1, CanESM5 has a small regional mean precipitation bias, but a weak pattern correlation, compared to APHRODITE. It has a particularly large dry bias over India, with less than 3 mm day^{-1} in the seasonal mean, and a relatively large excess of precipitation over the Tibetan Plateau and into China. MIROC6 performs relatively well over land, but has excessive precipitation west of India. Such biases may affect the pattern of the precipitation anomaly in the SSPs relative to the present day (Wilcox et al., 2015).

Aerosol optical depth (AOD) is a measure of the extinction of solar radiation due to scattering and absorption by an aerosol layer. Comparison of simulated and MODIS (Remer et al. (2008); Platnick (2015)) 550nm aerosol optical depth for the common 2002-2014 period, shows that models underestimate AOD over much of the tropics and NH mid-high latitudes, and overestimate it in the SH midlatitudes (Figure 4a-c). This pattern is common across models, with the exception of CanESM5, which overestimates AOD over Eurasia compared to MODIS (Supplementary Figure S6 shows the comparison between AOD from individual models and MODIS). AOD gives an indication of the amount of aerosol in a given location, but does not give an indication of aerosol forcing. It gives no indication of particle number, as AOD is influenced by the optical properties of those particles, and no indication of aerosol-cloud interactions, which account for the majority of aerosol forcing in models (Zelinka et al., 2014).

2.3 Future anthropogenic aerosol changes

In all SSPs the largest AOD changes are over Asia (Figure 4d-f), consistent with the changes in aerosol and precursor emissions (Figure 1). Future changes in AOD are characterised by global decreases in SSP1-1.9, with the exception of an initial increase over South Asia, and positive anomalies relative to 1980-2014 over the Tibetan Plateau and southern Africa, which may be dust (Figure 4d). AOD changes are characterised by regional contrasts in SSP2-4.5, with an overall decrease in the NH contrasted with an increase in the SH, and large decreases over East Asia against large increases over South Asia until the 2030s (Figure 4e). This Asian dipole pattern is persistent and strengthens from the present until the 2040s. In this pathway, the large increases in South Asian AOD are predominantly driven by increases in SO_2 emissions. SSP5-8.5 has similar aerosol changes to SSP2-4.5, consistent with the similar changes in emissions (Figure 1). The final scenario we consider, SSP3-7.0, also contrasts widespread decreases in NH AOD against increases in the SH (Figure 4f). However, this scenario also includes large aerosol and precursor emission and AOD increases over East Asia and particularly South Asia. These increases are driven predominantly by SO_2 over South Asia, but have a BC contribution over East Asia (Figure 1). This pattern persists, but the East Asian increase starts to weaken by 2050 (Figure 1).

3 Global response

Global mean annual mean temperature anomalies for 2025-2034, 2035-2044, and 2045-2054 relative to 1980-2014 are shown in Figure 5a. The boxes show the interquartile range, based on model mean responses, with individual model-mean responses overlaid. For each period, the responses are broadly ordered according to their GHG pathway, and diverge with time in a similar fashion to GHG emissions. This suggests that anthropogenic aerosol plays at most a limited role in the evolution of global mean near-surface temperature on these timescales, supporting the conclusions of Shindell and Smith (2019). However, as discussed later, it does play a role in the pattern and magnitude of regional temperature changes. Importantly, anthropogenic aerosol is the main driver of trends in the interhemispheric temperature gradient until 2050, which has a strong control on ITCZ position and the global monsoon, and thus regional precipitation (Figure 5d). There is a large spread across models, consistent with the large uncertainty in historical trends, but a monotonic increase in the magnitude of the anomaly from SSP3-7.0 to SSP1-1.9 is present in all three future periods. The dominant role of anthropogenic aerosol is further supported by the comparable magnitude of anomalies in SSP2-4.5 and SSP5-8.5.

There is a clear aerosol-driven signal in future increases in global mean precipitation and hydrological sensitivity (Figure 5b, c). There is the suggestion of the beginning of a shift towards GHGs as the dominant driver of precipitation increases in 2050, but this is not seen in hydrological sensitivity. where the SSP1-1.9 anomaly is marginally smaller than in SSP2-4.5. GHGs are the main driver of global precipitation change by the end of the 21st century (not shown).

4 Asian summer monsoon response

The decrease in Asian monsoon precipitation observed in the second half of the twentieth century has been attributed to the global increase in anthropogenic aerosols (Bollasina et al. (2011); Song et al. (2014); Polson et al. (2014)). The hemispheric asymmetry in aerosol forcing leads to an energy imbalance between the hemispheres, which in turn causes a slowdown of the meridional overturning circulation, and a weakening of the monsoon circulation (Bollasina et al. (2011); Song et al. (2014); Lau and Kim (2017); Undorf et al. (2018)). Local aerosol emissions further modify monsoon circulation and precipitation (Cowan and Cai (2011); Guo et al. (2015); Undorf et al. (2018)). In contrast to anthropogenic aerosols, where circulation changes are an important component of the response to forcing, GHGs mainly affect (increase) monsoon precipitation by enhancing tropospheric water vapour, and thus increasing moisture transport toward India (Li et al., 2015).

Global aerosol reductions in SSP1-1.9 briefly cause this scenario to warm faster than the others considered over Asia and East Asia, but this effect does not persist beyond the 2030s, and is not apparent over South Asia (Figure 6a). However, anthropogenic aerosol does affect the regional pattern of warming (Figure 7), with slower increases in land temperature in many areas in SSP2-4.5, 3-7.0, and 5-8.5 compared to SSP1-1.9. The growing influence of GHGs with time can also be seen in Figure 7 as greater warming in SSP5-8.5 compared to SSP2-4.5 over the ocean, and over land from 2040. Continued increases in anthropogenic aerosol emissions in SSP3-7.0 appear to moderate land warming compared to other SSPs, despite large GHG increases.

As for the global mean case (Figure 5), the influence of aerosol is more clearly seen in regional mean precipitation than regional mean temperature (Figure 6b). Over Asia, the largest mean precipitation increase occurs, for all decades, in SSP1-1.9,

the smallest increases in SSP3-7.0, and comparable changes in SSP2-4.5 and SSP5-8.5. The same pattern is found over East Asia for 2035-2044, but the picture is less clear for the other periods. This result could be a reflection of the role of internal variability or the transition to a period where precipitation increases are dominated by GHG changes, with East Asia warmer relative to present day in SSP2-4.5 and SSP5-8.5 compared to SSP1-1.9by the 2050s (Figure 6a, Figure 7. By 2100, GHGs are

5 the dominant influence on the relative magnitude of the future increases in Asian summer monsoon precipitation across the SSPs, as illustrated in Figure 8.

The pattern of the precipitation anomalies relative to 1980-2014 across the SSPs is very different over South Asia compared to East Asia and Asia as a whole (Figure 6). SSP1-1.9 and SSP3-7.0 both result in increases in precipitation relative to the present day, while precipitation changes are small in SSP2-4.5 and 5-8.5, especially in prior to the 2050s. The effect of increased

10 GHGs starts to become apparent by 2050, when larger precipitation increases are seen in SSP5-8.5 compared to SSP2-4.5 (Figure 6), consistent with the temperature response (Figure 7).

The AOD anomaly compared to 1980-2014 in SSP2-4.5 is characterised by a dipole between increases in South Asian AOD and decreases over East Asia. This pattern is present in observations since 2010 (Samset et al., 2019), and is in contrast to the twentieth century increases in both regions. The relatively small South Asian precipitation increases seen in SSP2-4.5

15 and SSP5-8.5 compared to SSP1-1.9 and SSP3-7.0, are likely to be due to suppressed warming over India due to continued anthropogenic aerosol increases there (Figure 1, 7). There is potential for this suppression to be enhanced by feedback between the East and South Asian monsoon system responses to forcing (Ha et al. (2018); Singh et al. (2019)).

Figures 9 and 10 show that the pattern of Asian precipitation changes are similar, regardless of the emission pathway that is followed, but that the magnitude of the changes are pathway dependent. Figure 9 shows the absolute anomaly compared to

20 1980-2014, while Figure 10 shows the anomaly relative to the SSP1-1.9 response. In Figure 10, the influence of GHGs can be seen, with greater GHG emissions driving greater drying over the Equatorial Indian Ocean and further increases in precipitation over India (particularly in the comparison between SSP2-4.5 and SSP5-8.5, and in SSP3-7.0 in the 2050s), as for temperature (Figure 7).

4.1 Aerosol only SSP2-4.5

25 Analysis of SSP2-4.5-aer, in which only anthropogenic aerosol emissions are varying with time following the SSP2-4.5 pathway, allows the response to aerosol changes to be isolated from that due to GHG changes. In this case, a dipole in temperature anomalies, with cooling over India and warming over East Asia, and in sea level pressure, with a positive anomaly over India, the Bay of Bengal, and the Indo-China peninsula, and a negative anomaly over the rest of Asia, can clearly be seen in both CanESM5 (Figure 11) and MIROC6 (Figure S7). This feature matches the dipole pattern in AOD changes, and is apparent in

30 the SSP2-4.5 response up to 2050 as a moderated GHG-induced warming over South Asian relative to East Asia (Figure 7). Differences in the character of the precipitation anomaly can be seen when comparing the anomalies pre- and post-2050. In the earlier periods, when South Asian aerosol emissions continue to increase, precipitation anomalies are either weakly positive or negative over India, the Bay of Bengal, and the Indo-China peninsula. Post-2050, when anthropogenic aerosols are decreasing throughout Asia, precipitation increases relative to 1980-2014. There are suggestions of this structure in the SSP2-4.5 response,

where increases in precipitation are weak over India and the Bay of Bengal compared to the SSP1-1.9 response (Figure 9, 10), but it is not as clear. This is likely partly due to the influence of GHG increases, and partly due to the effects of taking the mean response over models with large differences in their mean precipitation field (Figure 3; a number of the individual models do simulate a tripolar pattern in precipitation change in SSP2-4. 5 (Figure S8)).

5 Conclusions

There is large uncertainty in future anthropogenic aerosol emission pathways. This is likely to be of limited importance for global-mean temperature, but anthropogenic aerosol does play an important role in changes in regional temperature, and global and regional precipitation until 2050 under the Shared Socioeconomic Pathways. Rapid reductions in anthropogenic aerosol and precursor emissions in SSP1-1.9 lead to larger increases in global and Asian summer monsoon precipitation compared to SSP2-4.5, 3-7.0, and 5-8.5 over East Asia and especially South Asia.

In SSP2-4.5 anthropogenic aerosol continues to increase over South Asia, in contrast to decreases over East Asia. This leads to a suppressed precipitation increase over South Asia in SSP2-4.5 over the next 30 years in this scenario relative to SSP1-1.9 and SSP3-7.0. Such a dipole in aerosol trends over Asia has been observed over Asia since 2010, suggesting that SSP2-4.5 (where the current pattern persists) or SSP1-1.9 (where anthropogenic aerosol is reduced in both regions) are more likely than SSP3-7.0 (where anthropogenic aerosol increases in both regions). This presents the possibility of large uncertainty in South Asian summer monsoon precipitation on a 30-50 year time horizon due to uncertainty in aerosol emission pathways.

Data availability. All data used in this work are freely available for research purposes.

Author contributions. All authors designed the analysis and wrote the paper. LJW, ZL, BHS, EH, MTL, KN, and SU performed the analysis.

Competing interests. The authors declare that they have no conflict of interest.

Acknowledgements. This work and its contributors Laura Wilcox, Zhen Liu, and Massimo Bollasina were supported by the UK-China Research & Innovation Partnership Fund through the Met Office Climate Science for Service Partnership (CSSP) China as part of the Newton Fund. Laura Wilcox received additional support from the Natural Environment Research Council (NERC; grant NE/S004890/1) and the International Meteorological Institute (IMI) visiting scientist program.

We acknowledge the World Climate Research Programme, which, through its Working Group on Coupled Modelling, coordinated and promoted CMIP6. We thank the climate modelling groups for producing and making available their model output, the Earth System Grid Federation (ESGF) for archiving the data and providing access, and the multiple funding agencies who support CMIP6 and ESGF. APHRODITE

precipitation data are available from http://www.chikyu.ac.jp/precip. GISTEMP temperature data, and CMAP, GPCC, and GPCP precipitation data were provided by the NOAA/OAR/ESRL PSD, Boulder, Colorado, USA, from their website at https://www.esrl.noaa.gov/psd/. We also acknowledge the use of ERA-Interim data produced by ECMWF and provided by the British Atmospheric Data Centre and the National Centre for Atmospheric Science. The analysis in this work was performed on the JASMIN super-data-cluster (Lawrence et al., 2012).

5   JASMIN is managed and delivered by the UK Science and Technology Facilities Council (STFC) Centre for Environmental Data Archival (CEDA).

References

Acosta Navarro, J. C., Varma, V., Riipinen, I., Seland, Ø., Kirkevåg, A., Struthers, H., Iversen, T., Hansson, H. C., and Ekman, A. M. L.: Amplification of Arctic warming by past air pollution reductions in Europe, Nature Geoscience, 9, http://dx.doi.org/10.1038/ngeo2673, 2016.

5 Acosta Navarro, J. C., Ekman, A. M. L., Pausata, F. S. R., Lewinschal, A., Varma, V., Seland, Ø., Gauss, M., Iversen, T., Kirkevåg, A., Riipinen, I., Hansson, H. C., Navarro, J. C. A., Ekman, A. M. L., Pausata, F. S. R., Lewinschal, A., Varma, V., Seland, Ø., Gauss, M., Iversen, T., Kirkevåg, A., Riipinen, I., and Hansson, H. C.: Future Response of Temperature and Precipitation to Reduced Aerosol Emissions as Compared with Increased Greenhouse Gas Concentrations, Journal of Climate, 30, 939–954, https://doi.org/10.1175/JCLI-D-16-0466.1, http://journals.ametsoc.org/doi/10.1175/JCLI-D-16-0466.1, 2017.

10 Adler, R. F., Huffman, G. J., Chang, A., Ferraro, R., Xie, P.-P., Janowiak, J., Rudolf, B., Schneider, U., Curtis, S., Bolvin, D., Gruber, A., Susskind, J., Arkin, P., Nelkin, E., Adler, R. F., Huffman, G. J., Chang, A., Ferraro, R., Xie, P.-P., Janowiak, J., Rudolf, B., Schneider, U., Curtis, S., Bolvin, D., Gruber, A., Susskind, J., Arkin, P., and Nelkin, E.: The Version-2 Global Precipitation Climatology Project (GPCP) Monthly Precipitation Analysis (1979–Present), Journal of Hydrometeorology, 4, 1147–1167, https://doi.org/10.1175/1525-7541(2003)004<1147:TVGPCP>2.0.CO;2, http://journals.ametsoc.org/doi/abs/10.1175/ 15 1525-7541{%}282003{%}29004{%}3C1147{%}3ATVGPCP{%}3E2.0.CO{%}3B2, 2003.

Andrews, T., Forster, P. M., Boucher, O., Bellouin, N., and Jones, A.: Precipitation, radiative forcing and global temperature change, Geophysical Research Letters, 37, n/a–n/a, https://doi.org/10.1029/2010GL043991, http://doi.wiley.com/10.1029/2010GL043991, 2010.

Bartlett, R. E., Bollasina, M. A., Booth, B. B. B., Dunstone, N. J., Marenco, F., Messori, G., and Bernie, D. J.: Do differences in future sulfate emission pathways matter for near-term climate? A case study for the Asian monsoon, Climate Dynamics, 50, 1863–1880, 20 https://doi.org/10.1007/s00382-017-3726-6, http://link.springer.com/10.1007/s00382-017-3726-6, 2018.

Bellouin, N., Rae, J., Jones, A., Johnson, C., Haywood, J., and Boucher, O.: Aerosol forcing in the Climate Model Intercomparison Project (CMIP5) simulations by HadGEM2-ES and the role of ammonium nitrate, Journal of Geophysical Research, 116, D20 206, https://doi.org/10.1029/2011JD016074, http://doi.wiley.com/10.1029/2011JD016074, 2011.

Bellouin, N., Mann, G. W., Woodhouse, M. T., Johnson, C., Carslaw, K. S., and Dalvi, M.: Impact of the modal aerosol scheme GLOMAP-25 mode on aerosol forcing in the Hadley Centre Global Environmental Model, Atmospheric Chemistry and Physics, 13, 3027–3044, https://doi.org/10.5194/acp-13-3027-2013, https://www.atmos-chem-phys.net/13/3027/2013/, 2013.

Bellouin, N., Quaas, J., Gryspeerdt, E., Kinne, S., Stier, P., Watson Parris, D., Boucher, O., Carslaw, K., Christensen, M., Daniau, A., Dufresne, J., Feingold, G., Fiedler, S., Forster, P., Gettelman, A., Haywood, J., Lohmann, U., Malavelle, F., Mauritsen, T., McCoy, D., Myhre, G., Mülmenstädt, J., Neubauer, D., Possner, A., Rugenstein, M., Sato, Y., Schulz, M., Schwartz, S., Sourdeval, O., Storelvmo, 30 T., Toll, V., Winker, D., and Stevens, B.: Bounding global aerosol radiative forcing of climate change, Reviews of Geophysics, p. 2019RG000660, https://doi.org/10.1029/2019RG000660, https://onlinelibrary.wiley.com/doi/abs/10.1029/2019RG000660, 2019.

Bollasina, M. A., Ming, Y., and Ramaswamy, V.: Anthropogenic aerosols and the weakening of the South Asian summer monsoon., Science (New York, N.Y.), 334, 502–5, https://doi.org/10.1126/science.1204994, http://www.ncbi.nlm.nih.gov/pubmed/21960529, 2011.

Boucher, O., Randall, D., Artaxo, P., Bretherton, C., Feingold, G., Forster, P., Kerminen, V.-M., Kondo, Y., Liao, H., Lohmann, U., Rasch, P., 35 Satheesh, S., Sherwood, S., Stevens, B., and Zhang, X.-Y.: Clouds and Aerosols. In: Climate Change 2013: The Physical Science Basis. Contribution of Working Group I to the Fifth Assessment Report of the Intergovernmental Panel on Climate Change, Climate Change

2013: The Physical Science Basis. Contribution of Working Group I to the Fifth Assessment Report of the Intergovernmental Panel on Climate Change, 2013.

Chalmers, N., Highwood, E. J., Hawkins, E., Sutton, R., and Wilcox, L. J.: Aerosol contribution to the rapid warming of near-term climate under RCP 2.6, Geophysical Research Letters, 39, https://doi.org/10.1029/2012GL052848, http://doi.wiley.com/10.1029/2012GL052848, 2012.

Collins, M., AchutaRao, K., Ashok, K., Bhandari, S., Mitra, A. K., Prakash, S., Srivastava, R., and Turner, A.: Observational challenges in evaluating climate models, Nature Climate Change, 3, 940–941, https://doi.org/10.1038/nclimate2012, http://www.nature.com/articles/nclimate2012, 2013.

Cowan, T. and Cai, W.: The impact of Asian and non-Asian anthropogenic aerosols on 20th century Asian summer monsoon, Geophysical Research Letters, 38, n/a–n/a, https://doi.org/10.1029/2011GL047268, http://doi.wiley.com/10.1029/2011GL047268, 2011.

Dee, D. P., Uppala, S. M., Simmons, A. J., Berrisford, P., Poli, P., Kobayashi, S., Andrae, U., Balmaseda, M. A., Balsamo, G., Bauer, P., Bechtold, P., Beljaars, A. C. M., van de Berg, L., Bidlot, J., Bormann, N., Delsol, C., Dragani, R., Fuentes, M., Geer, A. J., Haimberger, L., Healy, S. B., Hersbach, H., Hólm, E. V., Isaksen, L., Kållberg, P., Köhler, M., Matricardi, M., McNally, A. P., Monge-Sanz, B. M., Morcrette, J.-J., Park, B.-K., Peubey, C., de Rosnay, P., Tavolato, C., Thépaut, J.-N., and Vitart, F.: The ERA-Interim reanalysis: configuration and performance of the data assimilation system, Quarterly Journal of the Royal Meteorological Society, 137, 553–597, https://doi.org/10.1002/qj.828, http://doi.wiley.com/10.1002/qj.828, 2011.

Dong, B., Sutton, R., Highwood, E., and Wilcox, L.: Preferred response of the East Asian summer monsoon to local and non-local anthropogenic sulphur dioxide emissions, Climate Dynamics, 46, https://doi.org/10.1007/s00382-015-2671-5, 2016.

Eyring, V., Bony, S., Meehl, G. A., Senior, C. A., Stevens, B., Stouffer, R. J., and Taylor, K. E.: Overview of the Coupled Model Intercomparison Project Phase 6 (CMIP6) experimental design and organization, Geoscientific Model Development, 9, 1937–1958, https://doi.org/10.5194/gmd-9-1937-2016, https://www.geosci-model-dev.net/9/1937/2016/, 2016.

Fläschner, D., Mauritsen, T., Stevens, B., Fläschner, D., Mauritsen, T., and Stevens, B.: Understanding the Intermodel Spread in Global-Mean Hydrological Sensitivity, Journal of Climate, 29, 801–817, https://doi.org/10.1175/JCLI-D-15-0351.1, http://journals.ametsoc.org/doi/10.1175/JCLI-D-15-0351.1, 2016.

Gillett, N. P. and Von Salzen, K.: The role of reduced aerosol precursor emissions in driving near-term warming, Environmental Research Letters, 8, 034 008, https://doi.org/10.1088/1748-9326/8/3/034008, http://stacks.iop.org/1748-9326/8/i=3/a=034008?key=crossref.5e0362958468b043159465bd9c0f913d, 2013.

Gillett, N. P., Shiogama, H., Funke, B., Hegerl, G., Knutti, R., Matthes, K., Santer, B. D., Stone, D., and Tebaldi, C.: The Detection and Attribution Model Intercomparison Project (DAMIP v1.0) contribution to CMIP6, Geoscientific Model Development, 9, 3685–3697, https://doi.org/10.5194/gmd-9-3685-2016, https://www.geosci-model-dev.net/9/3685/2016/, 2016.

Guo, L., Turner, A. G., and Highwood, E. J.: Impacts of 20th century aerosol emissions on the South Asian monsoon in the CMIP5 models, Atmospheric Chemistry and Physics, 15, 6367–6378, https://doi.org/10.5194/acp-15-6367-2015, https://www.atmos-chem-phys.net/15/6367/2015/, 2015.

Guo, L., Turner, A. G., Highwood, E. J., Guo, L., Turner, A. G., and Highwood, E. J.: Local and Remote Impacts of Aerosol Species on Indian Summer Monsoon Rainfall in a GCM, Journal of Climate, 29, 6937–6955, https://doi.org/10.1175/JCLI-D-15-0728.1, http://journals.ametsoc.org/doi/10.1175/JCLI-D-15-0728.1, 2016.

Gusain, A., Ghosh, S., and Karmakar, S.: Added value of CMIP6 over CMIP5 models in simulating Indian summer monsoon rainfall, Atmospheric Research, 232, 104 680, https://doi.org/10.1016/J.ATMOSRES.2019.104680, https://www.sciencedirect.com/science/article/pii/S0169809519307665{#}coi0005, 2020.

Ha, K.-J., Seo, Y.-W., Lee, J.-Y., Kripalani, R. H., and Yun, K.-S.: Linkages between the South and East Asian summer monsoons: a review and revisit, Climate Dynamics, 51, 4207–4227, https://doi.org/10.1007/s00382-017-3773-z, http://link.springer.com/10.1007/s00382-017-3773-z, 2018.

Hansen, J., Ruedy, R., Sato, M., and Lo, K.: GLOBAL SURFACE TEMPERATURE CHANGE, Reviews of Geophysics, 48, RG4004, https://doi.org/10.1029/2010RG000345, http://doi.wiley.com/10.1029/2010RG000345, 2010.

Hegerl, G. C., Brönnimann, S., Cowan, T., Friedman, A. R., Hawkins, E., Iles, C., Müller, W., Schurer, A., and Undorf, S.: Causes of climate change over the historical record, Environmental Research Letters, 14, 123 006, https://doi.org/10.1088/1748-9326/ab4557, https://iopscience.iop.org/article/10.1088/1748-9326/ab4557, 2019.

Hienola, A., Partanen, A.-I., Pietikäinen, J.-P., O'Donnell, D., Korhonen, H., Matthews, H. D., and Laaksonen, A.: The impact of aerosol emissions on the 1.5 °C pathways, Environmental Research Letters, 13, 044 011, https://doi.org/10.1088/1748-9326/aab1b2, http://stacks.iop.org/1748-9326/13/i=4/a=044011?key=crossref.038a7a508aa27527067e48e972e2db8e, 2018.

Huang, B., Thorne, P. W., Banzon, V. F., Boyer, T., Chepurin, G., Lawrimore, J. H., Menne, M. J., Smith, T. M., Vose, R. S., and Zhang, H.-M.: Extended Reconstructed Sea Surface Temperature, Version 5 (ERSSTv5): Upgrades, Validations, and Intercomparisons, Journal of Climate, 30, 8179–8205, https://doi.org/10.1175/JCLI-D-16-0836.1, http://journals.ametsoc.org/doi/10.1175/JCLI-D-16-0836.1, 2017.

Jones, G. S., Stott, P. A., and Christidis, N.: Attribution of observed historical near-surface temperature variations to anthropogenic and natural causes using CMIP5 simulations, Journal of Geophysical Research: Atmospheres, 118, 4001–4024, https://doi.org/10.1002/jgrd.50239, http://doi.wiley.com/10.1002/jgrd.50239, 2013.

Kirkevåg, A., Grini, A., Olivié, D., Seland, Ø., Alterskjær, K., Hummel, M., Karset, I. H. H., Lewinschal, A., Liu, X., Makkonen, R., Bethke, I., Griesfeller, J., Schulz, M., and Iversen, T.: A production-tagged aerosol module for Earth system models, OsloAero5.3 – extensions and updates for CAM5.3-Oslo, Geoscientific Model Development, 11, 3945–3982, https://doi.org/10.5194/gmd-11-3945-2018, https://www.geosci-model-dev.net/11/3945/2018/, 2018.

Klimont, Z., Kupiainen, K., Heyes, C., Purohit, P., Cofala, J., Rafaj, P., Borken-Kleefeld, J., and Schöpp, W.: Global anthropogenic emissions of particulate matter including black carbon, Atmospheric Chemistry and Physics, 17, 8681–8723, https://doi.org/10.5194/acp-17-8681-2017, https://www.atmos-chem-phys.net/17/8681/2017/, 2017.

Kloster, S., Dentener, F., Feichter, J., Raes, F., Lohmann, U., Roeckner, E., and Fischer-Bruns, I.: A GCM study of future climate response to aerosol pollution reductions, Climate Dynamics, 34, 1177–1194, https://doi.org/10.1007/s00382-009-0573-0, http://link.springer.com/10.1007/s00382-009-0573-0, 2010.

Lau, W. K.-M. and Kim, K.-M.: Competing influences of greenhouse warming and aerosols on Asian summer monsoon circulation and rainfall, Asia-Pacific Journal of Atmospheric Sciences, 53, 181–194, https://doi.org/10.1007/s13143-017-0033-4, http://link.springer.com/10.1007/s13143-017-0033-4, 2017.

Lawrence, B., Bennett, V. L., Churchill, J., Juckes, M., Kershaw, P., Oliver, P., Pritchard, M., and Stephens, A.: The JASMIN super-data-cluster, arXiv preprint arXiv:1204.3553, https://www.academia.edu/2871931/The{_}JASMIN{_}super-data-cluster, 2012.

Lenssen, N. J. L., Schmidt, G. A., Hansen, J. E., Menne, M. J., Persin, A., Ruedy, R., and Zyss, D.: Improvements in the GISTEMP Uncertainty Model, Journal of Geophysical Research: Atmospheres, 124, 6307–6326, https://doi.org/10.1029/2018JD029522, https://onlinelibrary.wiley.com/doi/abs/10.1029/2018JD029522, 2019.

Levy, H., Horowitz, L. W., Schwarzkopf, M. D., Ming, Y., Golaz, J.-C., Naik, V., and Ramaswamy, V.: The roles of aerosol direct and indirect effects in past and future climate change, Journal of Geophysical Research: Atmospheres, 118, 4521–4532, https://doi.org/10.1002/jgrd.50192, http://doi.wiley.com/10.1002/jgrd.50192, 2013.

Li, X., Ting, M., Li, C., Henderson, N., Li, X., Ting, M., Li, C., and Henderson, N.: Mechanisms of Asian Summer Monsoon Changes in Response to Anthropogenic Forcing in CMIP5 Models, Journal of Climate, 28, 4107–4125, https://doi.org/10.1175/JCLI-D-14-00559.1, http://journals.ametsoc.org/doi/10.1175/JCLI-D-14-00559.1, 2015.

Liepert, B. G., Feichter, J., Lohmann, U., and Roeckner, E.: Can aerosols spin down the water cycle in a warmer and moister world?, Geophysical Research Letters, 31, n/a–n/a, https://doi.org/10.1029/2003GL019060, http://doi.wiley.com/10.1029/2003GL019060, 2004.

Liepert, B. G., Previdi, M., Liepert, B. G., and Previdi, M.: Do Models and Observations Disagree on the Rainfall Response to Global Warming?, Journal of Climate, 22, 3156–3166, https://doi.org/10.1175/2008JCLI2472.1, http://journals.ametsoc.org/doi/10.1175/2008JCLI2472.1, 2009.

Liu, L., Shawki, D., Voulgarakis, A., Kasoar, M., Samset, B. H., Myhre, G., Forster, P. M., Hodnebrog, Ø., Sillmann, J., Aalbergsjø, S. G., Boucher, O., Faluvegi, G., Iversen, T., Kirkevåg, A., Lamarque, J.-F., Olivié, D., Richardson, T., Shindell, D., Takemura, T., Liu, L., Shawki, D., Voulgarakis, A., Kasoar, M., Samset, B. H., Myhre, G., Forster, P. M., Hodnebrog, Ø., Sillmann, J., Aalbergsjø, S. G., Boucher, O., Faluvegi, G., Iversen, T., Kirkevåg, A., Lamarque, J.-F., Olivié, D., Richardson, T., Shindell, D., and Takemura, T.: A PDRMIP Multimodel Study on the Impacts of Regional Aerosol Forcings on Global and Regional Precipitation, Journal of Climate, 31, 4429–4447, https://doi.org/10.1175/JCLI-D-17-0439.1, http://journals.ametsoc.org/doi/10.1175/JCLI-D-17-0439.1, 2018.

Lund, M. T., Myhre, G., Haslerud, A. S., Skeie, R. B., Griesfeller, J., Platt, S. M., Kumar, R., Myhre, C. L., and Schulz, M.: Concentrations and radiative forcing of anthropogenic aerosols from 1750 to 2014 simulated with the Oslo CTM3 and CEDS emission inventory, Geoscientific Model Development, 11, 4909–4931, https://doi.org/10.5194/gmd-11-4909-2018, https://www.geosci-model-dev.net/11/4909/2018/, 2018.

Menne, M. J., Williams, C. N., Gleason, B. E., Rennie, J. J., and Lawrimore, J. H.: The Global Historical Climatology Network Monthly Temperature Dataset, Version 4, Journal of Climate, 31, 9835–9854, https://doi.org/10.1175/JCLI-D-18-0094.1, http://journals.ametsoc.org/doi/10.1175/JCLI-D-18-0094.1, 2018.

Moss, R. H., Edmonds, J. A., Hibbard, K. A., Manning, M. R., Rose, S. K., van Vuuren, D. P., Carter, T. R., Emori, S., Kainuma, M., Kram, T., Meehl, G. A., Mitchell, J. F. B., Nakicenovic, N., Riahi, K., Smith, S. J., Stouffer, R. J., Thomson, A. M., Weyant, J. P., and Wilbanks, T. J.: The next generation of scenarios for climate change research and assessment, Nature, 463, 747–756, https://doi.org/10.1038/nature08823, http://www.nature.com/articles/nature08823, 2010.

Mulcahy, J. P., Jones, C., Sellar, A., Johnson, B., Boutle, I. A., Jones, A., Andrews, T., Rumbold, S. T., Mollard, J., Bellouin, N., Johnson, C. E., Williams, K. D., Grosvenor, D. P., and McCoy, D. T.: Improved Aerosol Processes and Effective Radiative Forcing in HadGEM3 and UKESM1, Journal of Advances in Modeling Earth Systems, 10, 2786–2805, https://doi.org/10.1029/2018MS001464, https://onlinelibrary.wiley.com/doi/abs/10.1029/2018MS001464, 2018.

Nordling, K., Korhonen, H., Räisänen, P., Alper, M. E., Uotila, P., O'Donnell, D., and Merikanto, J.: Role of climate model dynamics in estimated climate responses to anthropogenic aerosols, Atmospheric Chemistry and Physics, 19, 9969–9987, https://doi.org/10.5194/acp-19-9969-2019, https://www.atmos-chem-phys.net/19/9969/2019/, 2019.

O'Neill, B. C., Tebaldi, C., van Vuuren, D. P., Eyring, V., Friedlingstein, P., Hurtt, G., Knutti, R., Kriegler, E., Lamarque, J.-F., Lowe, J., Meehl, G. A., Moss, R., Riahi, K., and Sanderson, B. M.: The Scenario Model Intercomparison Project (ScenarioMIP) for CMIP6,

Geoscientific Model Development, 9, 3461–3482, https://doi.org/10.5194/gmd-9-3461-2016, https://www.geosci-model-dev.net/9/3461/2016/, 2016.

Partanen, A.-I., Landry, J.-S., and Matthews, H. D.: Climate and health implications of future aerosol emission scenarios, Environmental Research Letters, 13, 024 028, https://doi.org/10.1088/1748-9326/aaa511, http://stacks.iop.org/1748-9326/13/i=2/a=024028?key=crossref.92c5bb2bc9b2717c4d48fe03d3ba8af8, 2018.

Pietikäinen, J.-P., Kupiainen, K., Klimont, Z., Makkonen, R., Korhonen, H., Karinkanta, R., Hyvärinen, A.-P., Karvosenoja, N., Laaksonen, A., Lihavainen, H., and Kerminen, V.-M.: Impacts of emission reductions on aerosol radiative effects, Atmospheric Chemistry and Physics, 15, 5501–5519, https://doi.org/10.5194/acp-15-5501-2015, https://www.atmos-chem-phys.net/15/5501/2015/, 2015.

Platnick, S.: MODIS Atmosphere L3 Monthly Product, NASA MODIS Adaptive Processing System, https://doi.org/http://dx.doi.org/10.5067/MODIS/MYD08_M3.006, https://modaps.modaps.eosdis.nasa.gov/services/about/products/c6/MYD08{_}M3.html, 2015.

Polson, D., Bollasina, M., Hegerl, G. C., and Wilcox, L. J.: Decreased monsoon precipitation in the Northern Hemisphere due to anthropogenic aerosols, Geophysical Research Letters, 41, 6023–6029, https://doi.org/10.1002/2014GL060811, http://doi.wiley.com/10.1002/2014GL060811, 2014.

Prakash, S., Mitra, A. K., Momin, I. M., Rajagopal, E. N., Basu, S., Collins, M., Turner, A. G., Achuta Rao, K., and Ashok, K.: Seasonal intercomparison of observational rainfall datasets over India during the southwest monsoon season, International Journal of Climatology, 35, 2326–2338, https://doi.org/10.1002/joc.4129, http://doi.wiley.com/10.1002/joc.4129, 2015.

Rao, S., Klimont, Z., Smith, S. J., Van Dingenen, R., Dentener, F., Bouwman, L., Riahi, K., Amann, M., Bodirsky, B. L., van Vuuren, D. P., Aleluia Reis, L., Calvin, K., Drouet, L., Fricko, O., Fujimori, S., Gernaat, D., Havlik, P., Harmsen, M., Hasegawa, T., Heyes, C., Hilaire, J., Luderer, G., Masui, T., Stehfest, E., Strefler, J., van der Sluis, S., and Tavoni, M.: Future air pollution in the Shared Socio-economic Pathways, Global Environmental Change, 42, 346–358, https://doi.org/10.1016/J.GLOENVCHA.2016.05.012, https://www.sciencedirect.com/science/article/pii/S0959378016300723?via{%}3Dihub, 2017.

Remer, L. A., Kleidman, R. G., Levy, R. C., Kaufman, Y. J., Tanré, D., Mattoo, S., Martins, J. V., Ichoku, C., Koren, I., Yu, H., and Holben, B. N.: Global aerosol climatology from the MODIS satellite sensors, Journal of Geophysical Research, 113, D14S07, https://doi.org/10.1029/2007JD009661, http://doi.wiley.com/10.1029/2007JD009661, 2008.

Riahi, K., van Vuuren, D. P., Kriegler, E., Edmonds, J., O'Neill, B. C., Fujimori, S., Bauer, N., Calvin, K., Dellink, R., Fricko, O., Lutz, W., Popp, A., Cuaresma, J. C., KC, S., Leimbach, M., Jiang, L., Kram, T., Rao, S., Emmerling, J., Ebi, K., Hasegawa, T., Havlik, P., Humpenöder, F., Da Silva, L. A., Smith, S., Stehfest, E., Bosetti, V., Eom, J., Gernaat, D., Masui, T., Rogelj, J., Strefler, J., Drouet, L., Krey, V., Luderer, G., Harmsen, M., Takahashi, K., Baumstark, L., Doelman, J. C., Kainuma, M., Klimont, Z., Marangoni, G., Lotze-Campen, H., Obersteiner, M., Tabeau, A., and Tavoni, M.: The Shared Socioeconomic Pathways and their energy, land use, and greenhouse gas emissions implications: An overview, Global Environmental Change, 42, 153–168, https://doi.org/10.1016/J.GLOENVCHA.2016.05.009, https://www.sciencedirect.com/science/article/pii/S0959378016300681?via{%}3Dihub, 2017.

Rotstayn, L. D., Collier, M. A., Chrastansky, A., Jeffrey, S. J., and Luo, J.-J.: Projected effects of declining aerosols in RCP4.5: unmasking global warming?, Atmospheric Chemistry and Physics, 13, 10 883–10 905, https://doi.org/10.5194/acp-13-10883-2013, https://www.atmos-chem-phys.net/13/10883/2013/, 2013.

Rotstayn, L. D., Collier, M. A., and Luo, J.-J.: Effects of declining aerosols on projections of zonally averaged tropical precipitation, Environmental Research Letters, 10, 044 018, https://doi.org/10.1088/1748-9326/10/4/044018, http://stacks.iop.org/1748-9326/10/i=4/a=044018?key=crossref.5295dd98eb7c1dc839889ae968219dad, 2015.

Salzmann, M.: Global warming without global mean precipitation increase?, Science Advances, 2, e1501572, https://doi.org/10.1126/sciadv.1501572, http://advances.sciencemag.org/lookup/doi/10.1126/sciadv.1501572, 2016.

Samset, B. H., Myhre, G., Forster, P. M., Hodnebrog, Ø., Andrews, T., Faluvegi, G., Fläschner, D., Kasoar, M., Kharin, V., Kirkevåg, A., Lamarque, J., Olivié, D., Richardson, T., Shindell, D., Shine, K. P., Takemura, T., and Voulgarakis, A.: Fast and slow precipitation responses to individual climate forcers: A PDRMIP multimodel study, Geophysical Research Letters, 43, 2782–2791, https://doi.org/10.1002/2016GL068064, https://onlinelibrary.wiley.com/doi/abs/10.1002/2016GL068064, 2016.

Samset, B. H., Sand, M., Smith, C. J., Bauer, S. E., Forster, P. M., Fuglestvedt, J. S., Osprey, S., and Schleussner, C.-F.: Climate Impacts From a Removal of Anthropogenic Aerosol Emissions, Geophysical Research Letters, 45, 1020–1029, https://doi.org/10.1002/2017GL076079, http://doi.wiley.com/10.1002/2017GL076079, 2018.

Samset, B. H., Lund, M. T., Bollasina, M., Myhre, G., and Wilcox, L.: Emerging Asian aerosol patterns, Nature Geoscience, 12, 582–584, https://doi.org/10.1038/s41561-019-0424-5, http://www.nature.com/articles/s41561-019-0424-5, 2019.

Scannell, C., Booth, B. B. B., Dunstone, N. J., Rowell, D. P., Bernie, D. J., Kasoar, M., Voulgarakis, A., Wilcox, L. J., Acosta Navarro, J. C., Seland, Ø., and Paynter, D. J.: The Influence of Remote Aerosol Forcing from Industrialized Economies on the Future Evolution of East and West African Rainfall, Journal of Climate, 32, 8335–8354, https://doi.org/10.1175/JCLI-D-18-0716.1, http://journals.ametsoc.org/doi/10.1175/JCLI-D-18-0716.1, 2019.

Schneider, U., Becker, A., Finger, P., Meyer-Christoffer, A., Ziese, M., and Rudolf, B.: GPCC's new land surface precipitation climatology based on quality-controlled in situ data and its role in quantifying the global water cycle, Theoretical and Applied Climatology, 115, 15–40, https://doi.org/10.1007/s00704-013-0860-x, http://link.springer.com/10.1007/s00704-013-0860-x, 2014.

Shawki, D., Voulgarakis, A., Chakraborty, A., Kasoar, M., and Srinivasan, J.: The South Asian Monsoon Response to Remote Aerosols: Global and Regional Mechanisms, Journal of Geophysical Research: Atmospheres, 123, 11,585–11,601, https://doi.org/10.1029/2018JD028623, http://doi.wiley.com/10.1029/2018JD028623, 2018.

Shindell, D. and Smith, C. J.: Climate and air-quality benefits of a realistic phase-out of fossil fuels, Nature, 573, 408–411, https://doi.org/10.1038/s41586-019-1554-z, http://www.nature.com/articles/s41586-019-1554-z, 2019.

Shindell, D., Kuylenstierna, J. C. I., Vignati, E., van Dingenen, R., Amann, M., Klimont, Z., Anenberg, S. C., Muller, N., Janssens-Maenhout, G., Raes, F., Schwartz, J., Faluvegi, G., Pozzoli, L., Kupiainen, K., Höglund-Isaksson, L., Emberson, L., Streets, D., Ramanathan, V., Hicks, K., Oanh, N. T. K., Milly, G., Williams, M., Demkine, V., and Fowler, D.: Simultaneously mitigating near-term climate change and improving human health and food security., Science (New York, N.Y.), 335, 183–9, https://doi.org/10.1126/science.1210026, http://www.ncbi.nlm.nih.gov/pubmed/22246768, 2012.

Sillmann, J., Pozzoli, L., Vignati, E., Kloster, S., and Feichter, J.: Aerosol effect on climate extremes in Europe under different future scenarios, Geophysical Research Letters, 40, 2290–2295, https://doi.org/10.1002/grl.50459, http://doi.wiley.com/10.1002/grl.50459, 2013.

Singh, D., Bollasina, M., Ting, M., and Diffenbaugh, N. S.: Disentangling the influence of local and remote anthropogenic aerosols on South Asian monsoon daily rainfall characteristics, Climate Dynamics, 52, 6301–6320, https://doi.org/10.1007/s00382-018-4512-9, http://link.springer.com/10.1007/s00382-018-4512-9, 2019.

Smith, C. J., Forster, P. M., Allen, M., Leach, N., Millar, R. J., Passerello, G. A., and Regayre, L. A.: FAIR v1.3: a simple emissions-based impulse response and carbon cycle model, Geoscientific Model Development, 11, 2273–2297, https://doi.org/10.5194/gmd-11-2273-2018, https://www.geosci-model-dev.net/11/2273/2018/, 2018.

Song, F., Zhou, T., and Qian, Y.: Responses of East Asian summer monsoon to natural and anthropogenic forcings in the 17 latest CMIP5 models, Geophysical Research Letters, 41, 596–603, https://doi.org/10.1002/2013GL058705, http://doi.wiley.com/10.1002/2013GL058705, 2014.

Sperber, K. R., Annamalai, H., Kang, I.-S., Kitoh, A., Moise, A., Turner, A., Wang, B., and Zhou, T.: The Asian summer monsoon: an inter-comparison of CMIP5 vs. CMIP3 simulations of the late 20th century, Climate Dynamics, 41, 2711–2744, https://doi.org/10.1007/s00382-012-1607-6, http://link.springer.com/10.1007/s00382-012-1607-6, 2013.

Taylor, K. E., Stouffer, R. J., Meehl, G. A., Taylor, K. E., Stouffer, R. J., and Meehl, G. A.: An Overview of CMIP5 and the Experiment Design, Bulletin of the American Meteorological Society, 93, 485–498, https://doi.org/10.1175/BAMS-D-11-00094.1, http://journals.ametsoc.org/doi/abs/10.1175/BAMS-D-11-00094.1, 2012.

Undorf, S., Polson, D., Bollasina, M. A., Ming, Y., Schurer, A., and Hegerl, G. C.: Detectable Impact of Local and Remote Anthropogenic Aerosols on the 20th Century Changes of West African and South Asian Monsoon Precipitation, Journal of Geophysical Research: Atmospheres, 123, 4871–4889, https://doi.org/10.1029/2017JD027711, http://doi.wiley.com/10.1029/2017JD027711, 2018.

van Vuuren, D. P., Edmonds, J., Kainuma, M., Riahi, K., Thomson, A., Hibbard, K., Hurtt, G. C., Kram, T., Krey, V., Lamarque, J.-F., Masui, T., Meinshausen, M., Nakicenovic, N., Smith, S. J., and Rose, S. K.: The representative concentration pathways: an overview, Climatic Change, 109, 5–31, https://doi.org/10.1007/s10584-011-0148-z, http://link.springer.com/10.1007/s10584-011-0148-z, 2011.

Westervelt, D. M., Horowitz, L. W., Naik, V., Golaz, J.-C., and Mauzerall, D. L.: Radiative forcing and climate response to projected 21st century aerosol decreases, Atmospheric Chemistry and Physics, 15, 12 681–12 703, https://doi.org/10.5194/acp-15-12681-2015, https://www.atmos-chem-phys.net/15/12681/2015/, 2015.

Wilcox, L. J., Highwood, E. J., and Dunstone, N. J.: The influence of anthropogenic aerosol on multi-decadal variations of historical global climate, Environmental Research Letters, 8, 24 033, https://doi.org/10.1088/1748-9326/8/2/024033, 2013.

Wilcox, L. J., Dong, B., Sutton, R. T., and Highwood, E. J.: The 2014 hot, dry summer in northeast Asia, https://doi.org/10.1175/BAMS-D-15-00123.1, 2015.

Wu, P., Christidis, N., and Stott, P.: Anthropogenic impact on Earth's hydrological cycle, Nature Climate Change, 3, 807–810, https://doi.org/10.1038/nclimate1932, http://www.nature.com/articles/nclimate1932, 2013.

Wyser, K., van Noije, T., Yang, S., von Hardenberg, J., O'Donnell, D., and D{\"o}scher, R.: On the increased climate sensitivity in the EC-Earth model from CMIP5 to CMIP6, Geoscientisic Model Development Discussions, https://doi.org/https://doi.org/10.5194/gmd-2019-282, https://www.geosci-model-dev-discuss.net/gmd-2019-282/, 2019.

Xie, P., Arkin, P. A., Xie, P., and Arkin, P. A.: Analyses of Global Monthly Precipitation Using Gauge Observations, Satellite Estimates, and Numerical Model Predictions, Journal of Climate, 9, 840–858, https://doi.org/10.1175/1520-0442(1996)009<0840:AOGMPU>2.0.CO;2, http://journals.ametsoc.org/doi/abs/10.1175/1520-0442{%}281996{%}29009{%}3C0840{%}3AAOGMPU{%}3E2.0.CO{%}3B2, 1996.

Xie, P., Arkin, P. A., Xie, P., and Arkin, P. A.: Global Precipitation: A 17-Year Monthly Analysis Based on Gauge Observations, Satellite Estimates, and Numerical Model Outputs, Bulletin of the American Meteorological Society, 78, 2539–2558, https://doi.org/10.1175/1520-0477(1997)078<2539:GPAYMA>2.0.CO;2, http://journals.ametsoc.org/doi/abs/10.1175/1520-0477{%}281997{%}29078{%}3C2539{%}3AGPAYMA{%}3E2.0.CO{%}3B2, 1997.

Yatagai, A., Kamiguchi, K., Arakawa, O., Hamada, A., Yasutomi, N., Kitoh, A., Yatagai, A., Kamiguchi, K., Arakawa, O., Hamada, A., Yasutomi, N., and Kitoh, A.: APHRODITE: Constructing a Long-Term Daily Gridded Precipitation Dataset for Asia Based on a Dense

Network of Rain Gauges, Bulletin of the American Meteorological Society, 93, 1401–1415, https://doi.org/10.1175/BAMS-D-11-00122.1, http://journals.ametsoc.org/doi/abs/10.1175/BAMS-D-11-00122.1, 2012.

Zelinka, M. D., Andrews, T., Forster, P. M., and Taylor, K. E.: Quantifying Components of Aerosol-Cloud-Radiation Interactions in Climate Models, Journal of Geophysical Research: Atmospheres, 119, 7599–7615, https://doi.org/10.1002/2014JD021710, 2014.
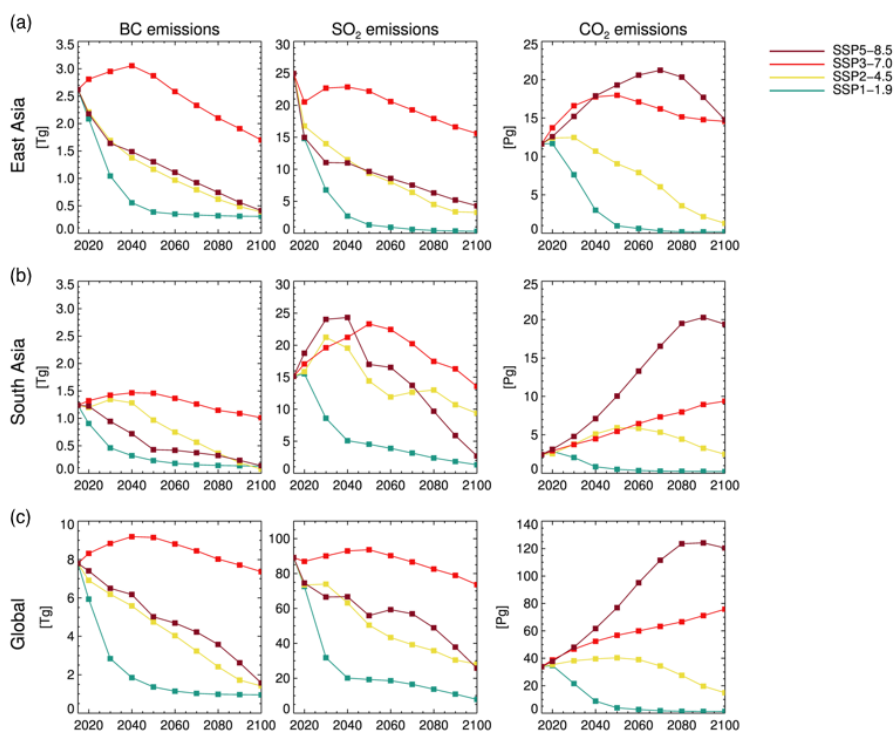
Figure 1. (a): Black carbon [Tg], (b): sulphur dioxide [Tg], and (c): carbon dioxide emissions [Pg] over East Asia for SSPs 1-19, 2-45, 3-70, and 5-85. (d)-(f): emissions over South Asia. (g)-(h): global total emissions. East Asia is the region from 100-120°E and 20-40°N. South Asia is the region from 55-95°E and 5-25°N.
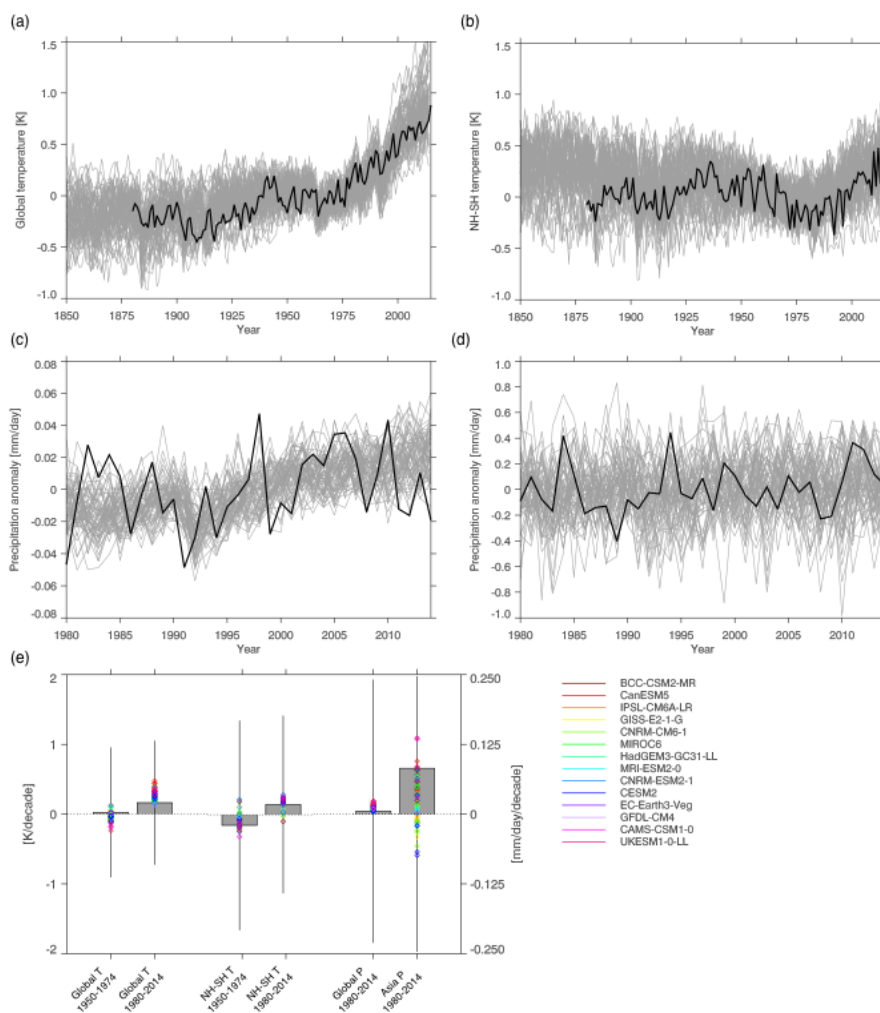
Figure 2. ((a): Global-mean annual-mean temperature anomaly relative to 1951-1980 from CMIP6 (grey lines show individual members) and GISTEMP (black). (b): June to August (JJA) mean interhemispheric temperature gradient anomaly relative to 1951-1980 from CMIP6 (grey) and GISTEMP. (c): Annual-mean global-mean precipitation anomaly relative to 180-2014 from CMIP6 (grey) and GPCP (black). (d): JJA mean Asia-mean precipitation anomaly relative to 1980-2014 from CMIP6 (grey) and GPCP (black). (e): linear trends in annual-mean global-mean temperature and JJA-mean interhemispheric temperature gradient from CMIP6 (coloured diamonds) and GISTEMP (grey bars) for 1950-1974 and 1980-2014, and linear trends in annual-mean global-mean precipitation and JJA-mean Asia-mean precipitation for 1980-2014. Error bars show plus or minus one standard error on the observed trend. Note that for Asian precipitation this extends beyond the range of the plot, and is an order of magnitude larger than the trend. Asia is the region from 67.5-145°E, and 5-47.5°N.
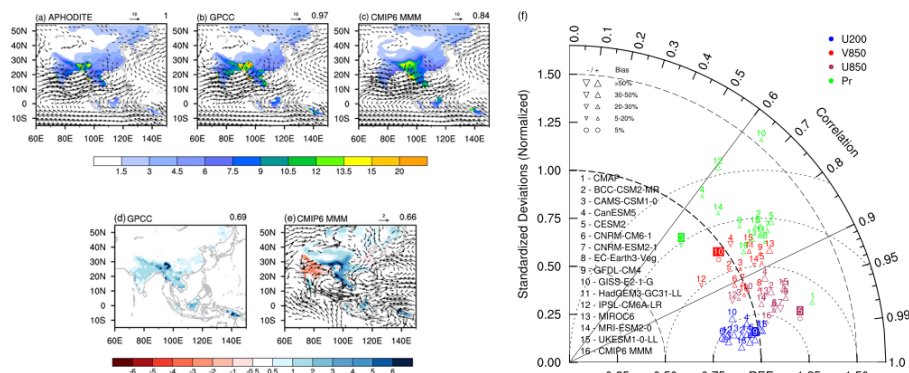
Figure 3. JJAS mean 1980-2014 mean precipitation over land overlaid with 850 hPa wind from (a): APHRODITE and ERA-Interim; (b): GPCC and ERA-Interim; (c): CMIP6 (multi-model mean). Values in the top right corner show the pattern correlation with APHRODITE precipitation. (d): Precipitation bias in GPCC relative to APHRODITE; (e): CMIP6 precipitation relative to APHRODITE and CMIP6 850 hPa winds relative to ERA-Interim. (f): Taylor diagram showing the relationship between individual CMIP6 models, the CMIP6 multi-model mean (point 16), and CMAP (point 1), with APHRODITE precipitation and ERA-Interim winds. Model numbers within a solid square indicate the model with the smallest absolute bias for each variable.
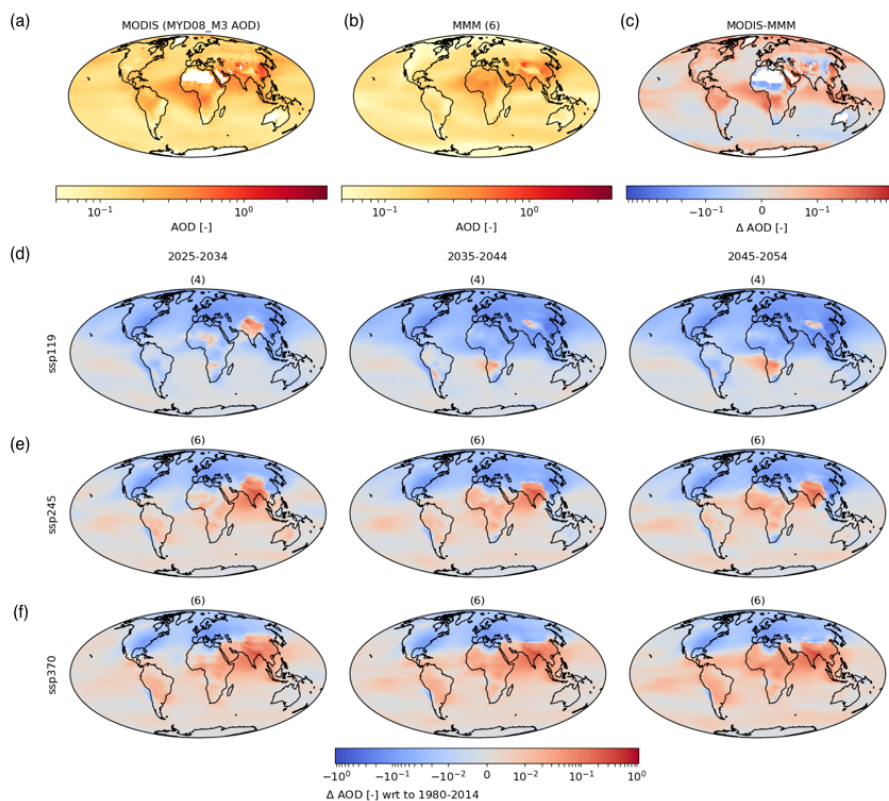
Figure 4. (a): 2002-2014 mean aerosol optical depth at 550 nm from MODIS; (b): 2002-2014 mean CMIP6 multi-model mean aerosol optical depth at 550 nm; (c): CMIP6 bias relative to MODIS. CMIP6 AOD anomalies for 2025-2034, 2035-2044, and 2045-2054 vs. 1980-2014 for (d): SSP1-1.9; (e): SSP2-4.5; and (f):SSP3-7.0. For SSP1-1.9 the anomalies are based on 4 models. For all other panels, 6 models are used (Table 1)
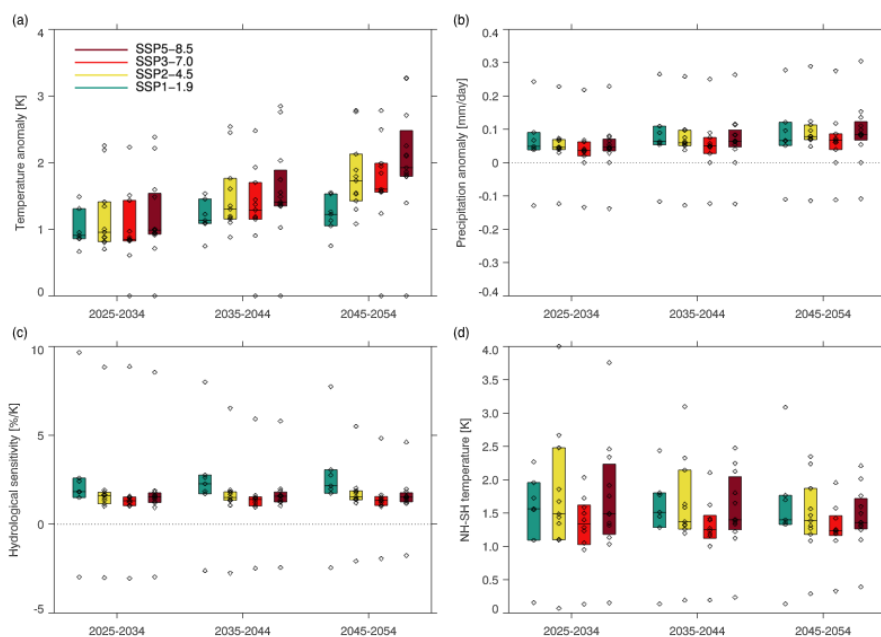
Figure 5. Global mean annual mean anomalies in (a): near-surface temperature [K]; (b): precipitation [mm/day]; (c): hydrological sensitivity [%/K] relative to 1980-2014. (d): JJA mean anomalies in interhemispheric temperature gradient [K] relative to 1980-2014.
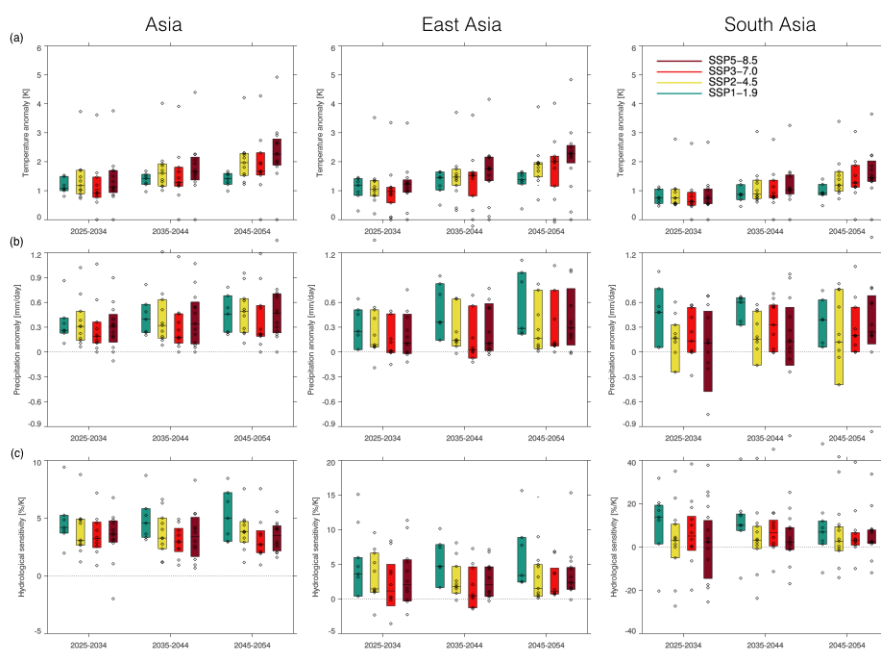
Figure 6. CMIP6 mean JJA mean temperature [K], precipitation [mm/day], and hydrological sensitivity [%/K] anomalies relative to 1980-2014 for (a): Asia; (b): East Asia; and (c): South Asia.
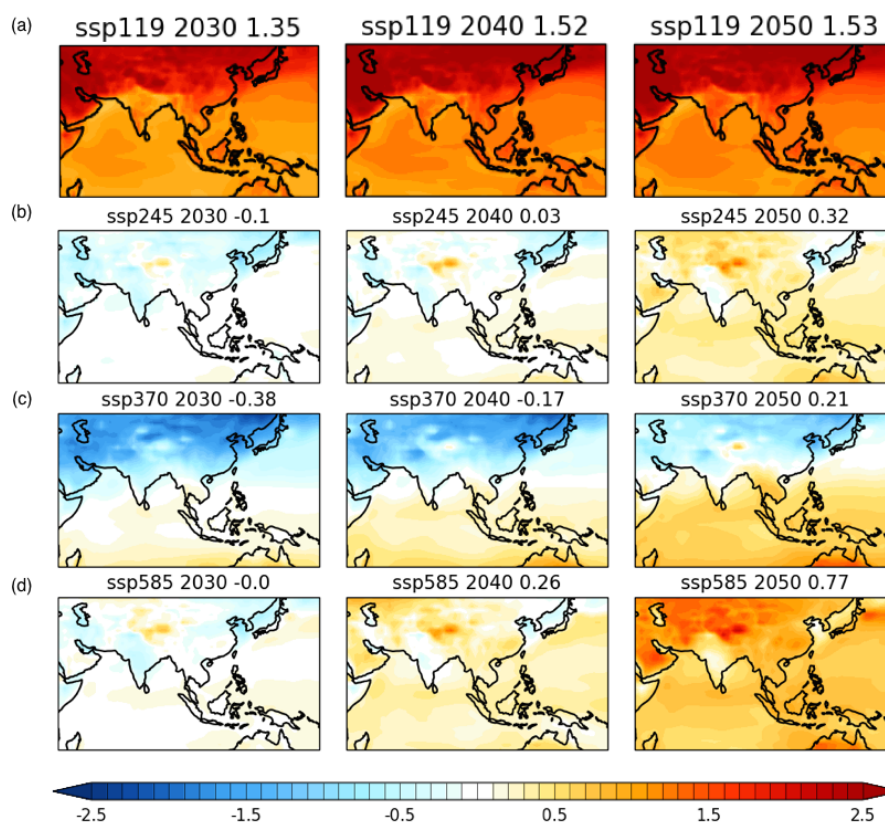
Figure 7. (a): CMIP6 JJAS near-surface temperature anomaly for 2025-2034, 2035-2044, and 2045-2054 vs. 1980-2014 from SSP1-1.9.
Relative anomalies for (b): SSP2-45.; (c): SSP3-7.0; and (d): SSP5-8.5 vs. SSP1-1.9.
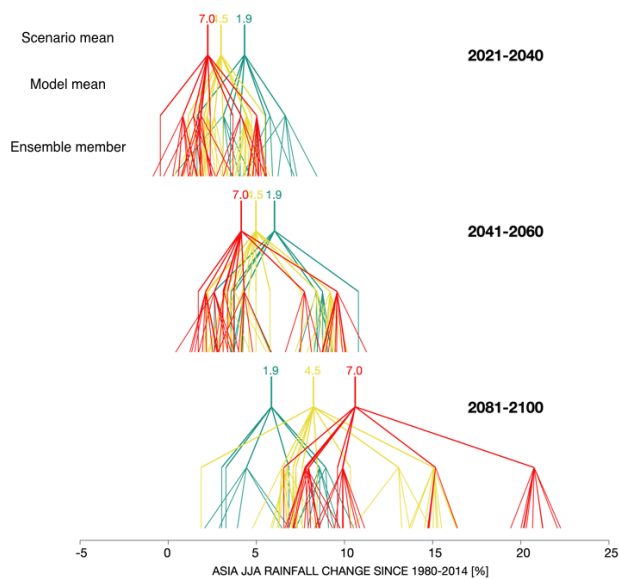
Figure 8. Asia mean JJA mean precipitation anomaly relative to 1980-2014 in individual models and ensemble members for 2021-2040, 2041-2060, and 2081-2100, from SSP1-1.9, SSP2-4.5, and SSP3-7.0.
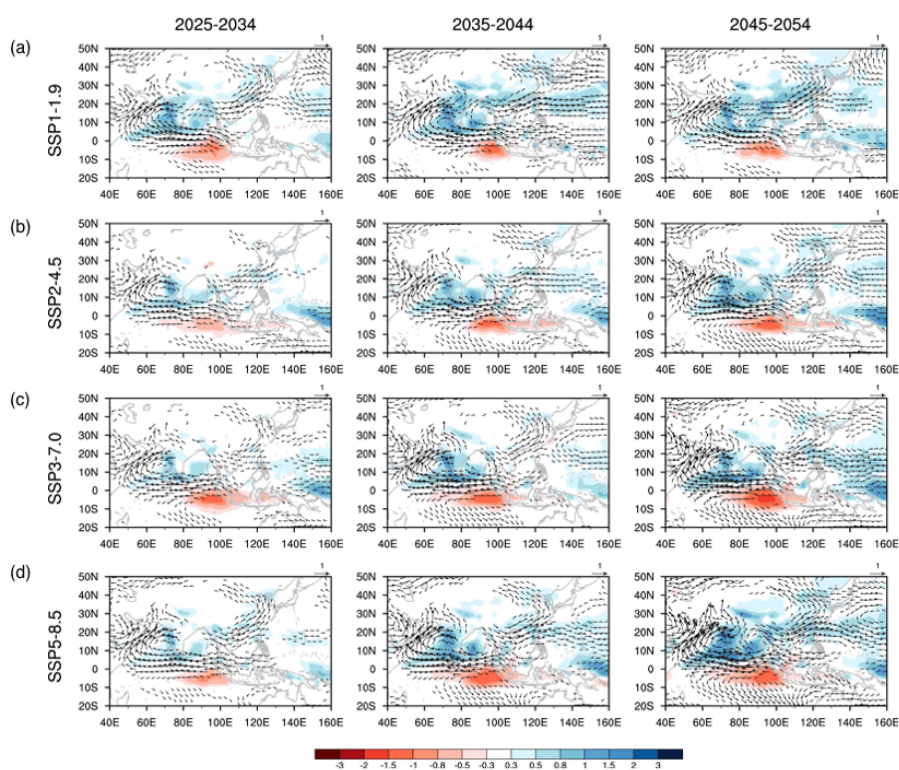
Figure 9. CMIP6 JJAS precipitation and 850 hPa wind anomalies for 2025-2034, 2035-2044, and 2045-2054 vs. 1980-2014 from (a): SSP1-1.9; (b): SSP2-4.5; (c): SSP3-7.0; and (d): SSP5-8.5.
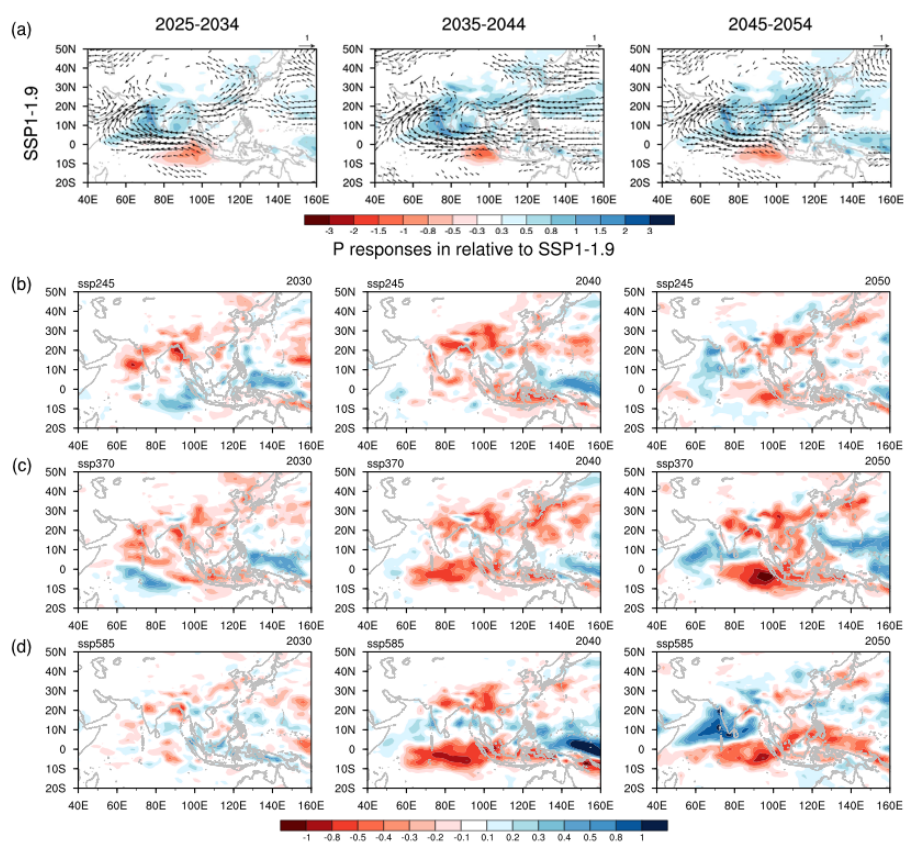
Figure 10. CMIP6 JJAS precipitation anomalies for 2025-2034, 2035-2044, and 2045-2054 vs. 1980-2014 from (a): SSP2-4.5; (b): SSP3-7.0; and (c): SSP5-8.5 relative to the anomalies from SSP1-1.9.
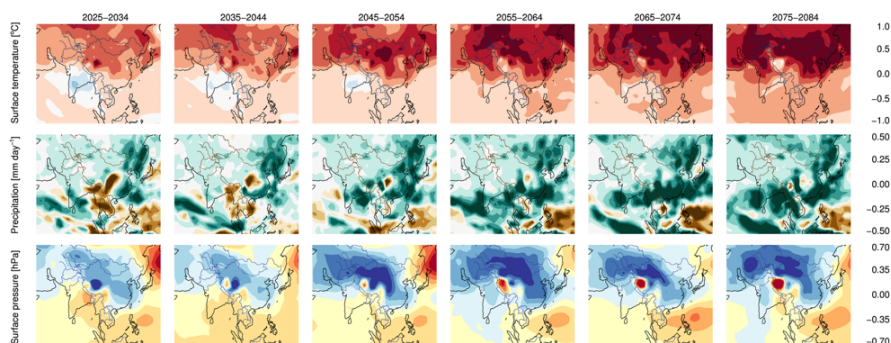
Figure 11. JJAS (a): near-surface temperature [K]; (b): precipitation [mm day^{-1}]; and (c): sea level pressure [hPa] anomalies for 10 year periods vs. 1980-2014 from an anthropogenic aerosol only version of SSP2-4.5 (SSP2-4.5-aer) with CanESM5.

Table 1. CMIP6 models, and the number of ensemble members for each, used in this work.

Centre	Model	AOD					T, P, U850, and V850				
		hist	1-1.9	2-4.5	3-7.0	5-8.5	hist	1-1.9	2-4.5	3-7.0	5-8.5
BCC	BCC-CSM2-MR						3		1	1	1
CAMS	CAMS-CSM1-0						1	1	1	1	1
CCCma	CanESM5	1	1	1	1	1	10	5	10	10	10
CNRM-CERFACS	CNRM-CM6-1	6		6	6	6	10		5	6	5
CNRM-CERFACS	CNRM-ESM2-1	5	5	5	5	5	5	5	5	5	
EC-Earth-Consortium	EC-Earth3-Veg						1		1		1
IPSL	IPSL-CM6A-LR	9	1	2	9	1	10	1	2	10	1
MIROC	MIROC6						3	1	3	3	3
MOHC	HadGEM3-GC31-LL						4				
MOHC	UKESM1-0-LL	6	5	5	5	5	4	4	5	5	5
MRI	MRI-ESM2-0						3	1	1	1	1
NASA-GISS	GISS-E2-1-G						5				
NCAR	CESM2	10		1	2	2	6		1	1	1
NOAA-GFDL	GFDL-CM4						1		1		1